AAPT PHYSICS EDUCATION | AMERICAN JOURNAL of PHYSICS

Galloping waves and their relativistic properties

William G. Harter, John Evans, Roberto Vega, and Sanford Wilson

Citation: American Journal of Physics **53**, 671 (1985); doi: 10.1119/1.14283
View online: http://dx.doi.org/10.1119/1.14283
View Table of Contents: http://scitation.aip.org/content/aapt/journal/ajp/53/7?ver=pdfcov
Published by the American Association of Physics Teachers

Galloping waves and their relativistic properties

William G. Harter
Theoretical Division, T-12, Los Alamos National Laboratory, Los Alamos, New Mexico 87545

John Evans, Roberto Vega, and Sanford Wilson
School of Physics, Georgia Institute of Technology, Atlanta, Georgia 30332

(Received 11 April 1983; accepted for publication 14 June 1984)

The superposition and resulting interference of two oppositely moving waves generally yield a wave having nonuniform motion. Space-time plots of constant-phase points provide a convenient way to exhibit a range of different types of wave phenomena including the relationship between moving and standing waves. Doppler-shifted versions of the same plots provide a novel approach to Minkowski graphs and Lorentz transformations. Relativistic properties of interfering electromagnetic plane waves are discussed.

I. INTRODUCTION

Some surfers, sailors, or others familiar with waves in water may recall seeing waves which move quite nonuniformly, indeed, they appear to gallop. The effect is most clearly seen when two wave trains of nearly equal amplitude meet head-on. For example, one may see waves appearing to gallop toward certain types of beaches which reflect a significant fraction of incoming waves, or they may occur in deep water between two passing yachts. Galloping wave motion is present in many other types of wave phenomena, however its transitory nature can make it hard to demonstrate. Hence it has been seldom if ever brought up in discussions of motion.

The galloping motion is a subtle effect associated with elementary wave interference between incident and reflected waves, and it should be of interest to instructors and students of elementary wave physics. It happens that *most* waves caused by a single frequency source have a galloping motion. The only exceptions are the very special cases of absolutely pure moving waves or absolutely pure standing waves. Unfortunately, it is these special cases which receive a disproportionate amount of attention in most elementary physics courses.[1]

On the other hand, many electrical engineering courses immediately introduce the concept and utility of interfering counter propagating waves. Engineering students learn that if a single frequency signal wave is sent along a transmission line to a load, the reflected wave interferes with the signal to make a standing wave pattern. By measuring the pattern's position and shape, i.e., its phase shift and standing wave ratio (SWR), one can determine the load impedance.

Physics students should be exposed to these elementary concepts, as well. In addition they may be curious enough to ask more detailed questions such as, What is the wave really doing *within* that standing wave pattern? How fast is it going? Can light waves do that, too? If so, what sort of motion could moving observers see or transcribe?

These questions came up in a senior level physics class at Georgia Tech, and they led the professor and students to explore some details of wave motion more thoroughly than is usual. It was found that the motion of a galloping wave could be related to a number of elementary and advanced concepts in optics, relativity, and quantum mechanics. There seemed to be a number of fascinating analogies and pedagogical visualization aids as well as unexplored possibilities. Among these possibilities are related interference effects which occur in two-dimensional wavefronts. Berry[2] has studied related effects involving wavefront "catastrophes" in acoustical measurements done on the ice shelf in Antarctica.[2]

II. STANDING WAVE PATTERNS AND GALLOPING MOTION

Suppose that a single frequency wave is going left to right down a transmission line while a reflected wave with half the amplitude is coming back. (This is the same as having one quarter of the input wave energy reflected.) A series of snapshots of the resulting wave amplitude is shown at the top of Fig. 1(a). The boundary or envelope of the waves is called the standing wave or modulation pattern. A time exposure would reveal a blur of waves which would fill in this pattern, but the pattern itself remains sharply defined and stationary for all time.

The snapshots reveal something about how the wave actually moves through its pattern. One can see that the wave amplitude rises and falls as the two counter propagating waves interfere. Furthermore, while the wave amplitude is near its maximum value the wave slows down as though it were an animal pausing to catch its breath. At this moment the successive zero points of the larger wave snapshots are much closer to each other than they are for the smaller ones despite the fact that the time interval between snapshots is equal in all cases. Finally, as the wave amplitude nears its minimum value the wave accelerates or gallops through the constricted part of the standing wave envelope at a much greater speed, and then it slows down to repeat the process.

A succession of snapshots are plotted one above the preceding one in the lower portion of Fig. 1(a). One can view this as a three-dimensional plot in which each wave amplitude is plotted on a reduced scale normal to a space (x)-time (ct) plane. (Here c denotes the wave phase velocity.) The main purpose of the plot is to show space-time trajectories of the wave zero points where each wave intersects the plane. The trajectories are the bolder lines which look like staircases ascending from left to right in Fig. 1. The slope $(\dot{x})$ measured at any point (x, t) along the space-time trajectory plots is the instantaneous zero-point speed. For a pure moving wave (no reflection) the zero trajectories would all be straight lines of constant slope-c in the (x, t) plane or unit slope in the (x, ct) plane of Fig. 1. As it is, they oscillate around the unit or 45° slope as the wave gallops off to the right.

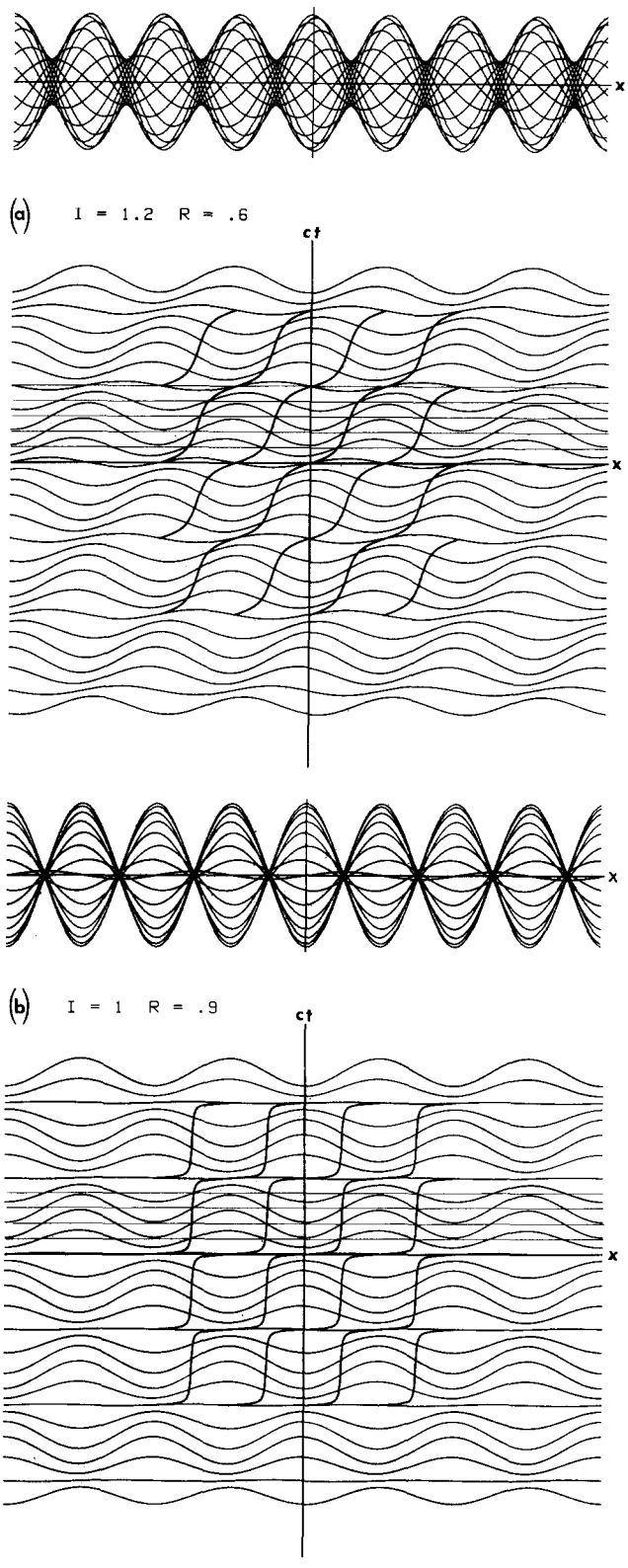

Fig. 1. Space-time trajectories of the zero points of a galloping wave for two values of the standing wave ratio. (a) SWR $= \Delta = 1/3$, (b) SWR $= \Delta = 1/19$. Waveforms for equal time intervals are superimposed at the top of each figure.

The galloping effect increases as the amplitude of the reflected wave approaches that of the incident wave. Figure 1(b) shows snapshots and space-time plots of a wave in which the reflected wave amplitude is 90% that of the incident wave. One can see that for long periods of time the wave zeros and crests are creeping along at a speed that is a small fraction of the normal phase velocity (c). In between these resting periods the wave briefly shrinks and gallops through the neck of the SWR pattern at a speed that is many times c. The galloping is just sufficient to make up for time lost during the resting periods, and the average speed of the waves can be seen to exactly equal the phase velocity c in Fig. 1.

It is convenient to parameterize the galloping waves with the standing wave ratio (SWR $= \Delta$) defined by

$$\Delta = (I - R)/(I + R)\,, \tag{2.1}$$

where I and R are amplitudes of incident and reflected waves, respectively. The Δ is simply the ratio of the minima and maxima in the standing wave pattern. The usual SWR definition is actually the inverse of Eq. (2.1), but we prefer not to deal with infinite ratios. The form of the wavecrest or wave-zero trajectories is shown for a range of SWR values in Fig. 2. One can see a smooth transition between trajectories of pure right-moving waves (SWR $= \Delta = 1.0$) on the left-hand side of Fig. 2, pure standing waves ($\Delta = 0$) in the center of Fig. 2, and pure left-moving waves ($\Delta = -1$) on the right-hand side. [Note that the waves with negative SWR (i.e., $R > I$) have more energy coming from the right-hand side than is going toward it.] The waves with noninteger Δ (i.e., most waves) have zero-point trajectories that resemble staircases. As Δ approaches zero the up and down bends in the staircases approach each other to form what will be called avoided crossings. At precisely $\Delta = 0$ the crossings are completed and a square grid of trajectories occurs for the standing wave case in Fig. 2.

One can easily show that the maximum zero-point speed of a galloping wave is inversely proportional to the SWR value Δ. Giving the wave amplitude in complex form

$$A(x, t) = (I e^{ikx} + Re^{-ikx})\, e^{-i\omega t}\,, \tag{2.2}$$

one has only to locate the zeros of the real part of this wave function. For now let I and R be real. Then

$$\begin{aligned}\mathrm{Re}\, A(x, t) &= (I + R)\cos(kx)\cos(\omega t) \\ &\quad + (I - R)\sin(kx)\sin(\omega t) = 0\,.\end{aligned} \tag{2.3}$$

This yields an equation for zero-point space-time trajectories.

$$\tan(kx) = -(1/\Delta)\cos(\omega t)\,. \tag{2.4}$$

This equation and its derivative yield the wave speed

$$v_{\text{zero}} = c\Delta/[\Delta^2 + (1 - \Delta^2)\cos^2(\omega t)]\,, \tag{2.5a}$$

$$= c/\Delta\,, \text{ when } \omega t = \pi/2, 3\pi/2, \ldots, \tag{2.5b}$$

$$= c\Delta\,, \text{ when } \omega t = 0, \pi\,, \tag{2.5c}$$

where

$$\omega/k = c \tag{2.5d}$$

is the usual expression for wave phase velocity.

A plot of the velocity function (2.5a) is shown in Fig. 3 for two different values of SWR. As Δ decreases the peaks turn into higher and sharper spikes. The area under each spike represents the distance through which the wave gallops in each period, and this is a constant. Therefore, as $\Delta \to 0$ each spike becomes a Dirac delta function multiplied by a constant.

The fact that the zero-point speed of galloping waves oscillates above and below the phase velocity (c) leads to some interesting relativistic kinematics in the case of light for which 2.99792458×10^2 cm/s. This effect provides one

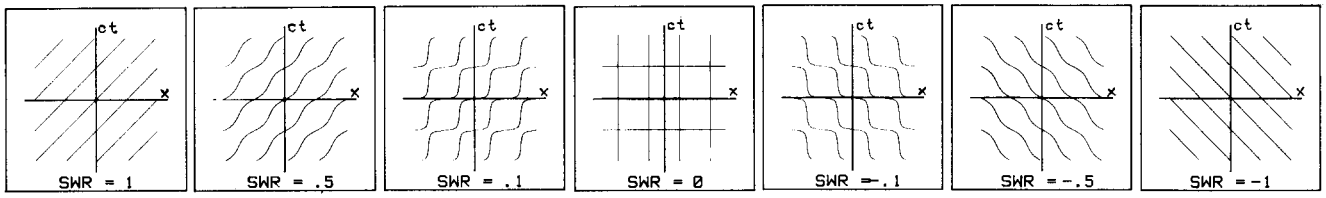

Fig. 2. Wave zero-point trajectories for a range of standing wave ratios.

of the simplest one-dimensional examples of a measurable phenomenon which travels faster than light. In principle, even sound or water waves could be made to temporarily exceed the speed of light in this way.

While these effects cannot be used to superluminally transmit energy, matter, or information, they might provide a practical space-time measuring system for certain prearranged relativistic experiments. Also, as discussed in Secs. IV and V, they provide kinematic thought experiments which illuminate an old relativistic curiosity. This curiosity concerns the view in different rest frames of anything which temporarily exceeds the speed of light. Some rest frames must for a moment see three copies of this "thing" in the form of two "things" propagating normally and one "antithing" propagating backwards in time. In other words, the trajectory becomes a space-time switch-back path, and it is analogous to certain Feynman diagrams of electron paths in Compton scattering.[3]

Before discussing the relativistic view of galloping waves, we shall relate them to some more commonly observed types of interference effects and oscillatory phenomena which appear in modern physics.

III. COMPARISON OF GALLOPING WITH OTHER OSCILLATORY PHENOMENA

By considering interference of two arbitrary one-dimensional waves, one can discuss several different effects. Let the wave function have the form

$$\psi(x,t) = A\, e^{i(k_a x - \omega_a t)} + B\, e^{i(k_b x - \omega_b t)}, \tag{3.1a}$$

where the angular frequencies

$$\omega_a = 2\pi\nu_a\ ,\ \omega_b = 2\pi\nu_b \tag{3.1b}$$

and wavenumbers or wave vectors

$$|k_a| = 2\pi/\lambda_a\ ,\ |k_b| = 2\pi/\lambda_b \tag{3.1c}$$

may now have different magnitudes as may also the wave amplitudes

$$A = A\, e^{i\alpha}\ ,\ B = B\, e^{i\beta}\ . \tag{3.1d}$$

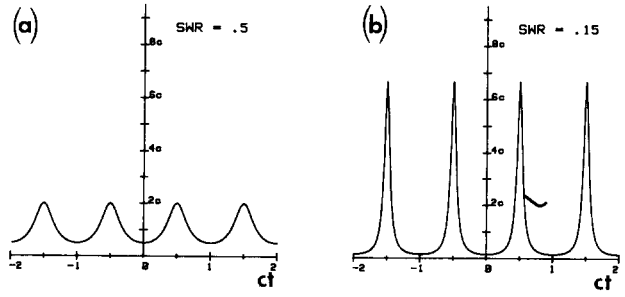

Fig. 3. Dependence of galloping wave velocity for two values of the standing wave ratio. (a) SWR $= \Delta = 1/2$, (b) SWR $= \Delta = 3/20$.

For many applications of wave mechanics one is interested in the envelope or modulation function $M(x,t)$ which determines the maximum amplitude at each point in space and time. Also, one finds the intensity or energy density to be proportional to M^2. The modulus $M(x,t)$ of the wave (3.1) is the square root of the absolute square of ψ, i.e.,

$$\begin{aligned} M(x,t) &= [\psi^*\psi]^{1/2}\ , \\ M(x,t) &= \left[\left(Ae^{-i(k_a x - \omega_a t + \alpha)} + Be^{-i(k_b x - \omega_b t + \beta)}\right) \right. \\ &\quad \left. \times \left(Ae^{i(k_a x - \omega_a t + \alpha)} + Be^{i(k_b x - \omega_b t + \beta)}\right) \right]^{1/2}\ , \\ M(x,t) &= \{A^2 + B^2 + 2AB\cos[(k_a - k_b) \\ &\quad \times x - (\omega_a - \omega_b)t + \alpha - \beta]\}^{1/2}\ . \end{aligned} \tag{3.2}$$

The galloping wave envelopes are a special case of this formula in which the frequencies of the A and B waves are equal, that is,

$$\omega \equiv \omega_a = \omega_b\ , \tag{3.3a}$$

and the wave vectors have equal magnitude but opposite direction or sign,

$$\begin{aligned} k &\equiv k_a = -k_b \\ &= \omega/c\ . \end{aligned} \tag{3.3b}$$

For this case one obtains from Eqs. (3.2) and (3.3) the modulus

$$M(x,\cdot) = [A^2 + B^2 + 2AB\cos(2kx + \alpha - \beta)]^{1/2}\ . \tag{3.4}$$

This is the equation for the envelopes of the standing wave patterns in the upper portions of Fig. 1(a) and (b). (For this we set $I = A$ and $R = B$ and let $\alpha = 0 = \beta$.) The envelopes are indeed standing patterns since (3.4) is independent of time. Where they stand depends on the phase difference $(\alpha - \beta)$ between the two interfering A and B waves. One should note that the minima of the M function are sharper than the maxima. Engineers find that more accurate measurements of the location of standing patterns are made at their minima. For zero SWR ($A = B = I = R$, and $\Delta = 0$) the minima collapse to zero and the envelope becomes a simple cosine function

$$\begin{aligned} M(x,\cdot) &= 2I\left[\tfrac{1}{2} + \tfrac{1}{2}\cos(2kx + \alpha - \beta)\right]^{1/2} \\ &= 2I\cos[kx + (\alpha - \beta)/2]\ . \end{aligned} \tag{3.5}$$

This defines the envelope of a pure standing wave.

A. Amplitude modulation and beating

The phenomena associated with "beats" and amplitude modulation (AM) arise when the A and B wave vectors have the same sign but differ in magnitude by some amount

$$\delta k \equiv k_a - k_b\ . \tag{3.6}$$

Generally, this means the angular frequencies of the two

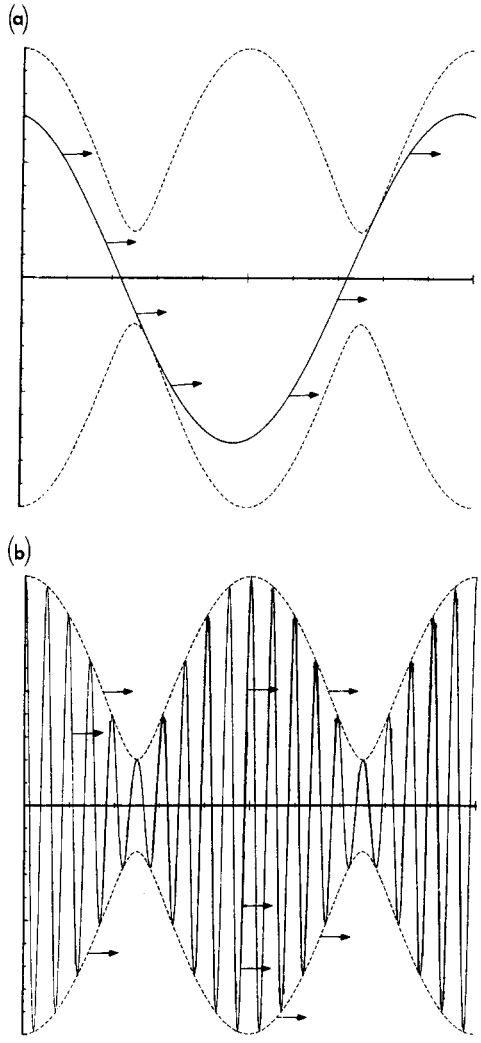

Fig. 4. Two different kinds of waves bounded by the same modulation envelopes. (a) Galloping waves with standing wave ratio SWR $= \Delta = 1/5$. Envelope is stationary. (b) Amplitude modulation with modulation factor $\mu = 1/5$. Envelope moves rigidly with the internal carrier wave in the absence of dispersion.

waves also differ by some amount

$$\delta\omega \equiv \omega_a - \omega_b \,. \tag{3.7}$$

From Eq. (3.2) it follows that the resulting wave oscillations are contained within modulation function (M) envelopes that have the same shape as the ones for galloping waves.

However, there are some important differences. One difference is that a wave with small $\delta\omega$ may pack many oscillations into one lump of the M function where there can only be one-half of a galloping wave. This comparison is made in Fig. 4 between a galloping wave plot versus x at an instant t and a similar plot of a small $\delta\omega$ wave. (Both waves have the same ratio of amplitudes A to B.) The oscillation associated with each M-function lump in Fig. 4(b) is called *beating* or amplitude modulation (AM). Where one uses the SWR(Δ) to describe galloping one instead describes AM by a similarily defined *modulation factor*

$$\mu = (A - B)/(A + B) \tag{3.8}$$

or by a modulation percentage $p = 100(1 - \mu)$.

Another difference between galloping and beating is that the M function for beating waves is a moving rather than a standing pattern. It follows from Eqs. (3.2), (3.6), and (3.7) that the pattern moves with velocity

$$v_g = \frac{\delta\omega}{\delta k}, \tag{3.9}$$

which is called the *group velocity*. If the speed of waves is independent of frequency, that is, if there is no dispersion, then v_g is simply equal to be phase velocity c. Therefore, nondispersive beating involves uniform motion of a rigid wave pattern such as is shown in Fig. 4(b), and this is quite unlike the motion associated with nondispersive galloping.

It is possible to have a mixture of beating and galloping by involving a pair of interfering waves whose wave vectors differ in magnitude *and* sign. However, we find it more illuminating to consider this situation in the context of relativistic optical Doppler effects. This is discussed in Secs. IV and V.

B. Polarization ellipsometry and other two-state oscillating systems

The mechanics of the two-state quantum system is indispensible to anyone studying modern quantum optics. This was originally developed by Rabi, Ramsey, and Schwinger[4] for describing the two states (spin-up and spin-down) involved in the magnetic resonance of an electron or proton. It was extended to arbitrary two-level systems by Feynman, Vernon, and Hellwarth[5] and this provides a basis for a multitude of effects involving maser and laser dynamics.

It is instructive to search for two-state systems which are less abstract and pedagodigically more accessible to students of wave mechanics and quantum theory. One such system involves the polarization states of electromagnetic plane waves. Plane waves in the most general elliptically polarized state may be expressed as complex linear combinations of a pair of right and left circularly polarized base states or else as a combination of x- and y-plane polarized states. Another such system involves all possible waves of a single frequency propagating in one dimension. We have already noted that a galloping wave such as (2.2) may be expressed as a (in general complex) combination of two oppositely moving waves.

The advantages of relating two-state mechanics to polarization ellipsometry are described in an earlier AJP article.[6] Galloping waves provide an even more elementary example of a two-state model. One can easily show that right and left circularly polarized states in a polarization model correspond directly to right and left moving waves in a wave model. Similarly, x- and y-plane polarized states correspond to cosine and sine standing waves. For each member of the continuum of elliptically polarized states there is a corresponding galloping wave state. The quantity which gallops in the polarization ellipse is the polar phase angle, and this galloping becomes more accentuated for more eccentric ellipses, i.e., for $\Delta \to 0$.

Modern quantum physics of atoms, molecules, and solids contain many examples of two-state models which exhibit some form of galloping. Molecular orbitals on rotating molecules or in the presence of magnetic fields have eigenstates which are neither pure moving nor pure standing waves but some galloping combination. Orbital quenching involves the continuous transformation of moving waves into standing waves.

The evolution of nonstationary quantum states often in-

volves passing through a galloping phase. For example, it would be wonderful to have a movie of the evolution of certain initially pure moving waves whose energy lies above the top of a periodic potential barrier. The wave would continuously evolve through the states represented by Fig. 2 going from one side to the other and back again. This would show that ideal barrier *reflection* or Bragg scattering occurs continuously through wave *galloping*. On the other hand, Feynman[7] has emphasized in his text that barrier *tunneling* between potential wells occurs continuously through *beating*. Together these two examples provide a vivid and complimentary picture of the quantum dynamics in periodic potentials.

Many problems in the quantum theory of scattering are also generalizations of the engineer's transmission line and load problem, and, as such, involve galloping waves. This is particularly true for one-dimensional potential scattering problems. If one shows students the details of the phases and wave motion in scattering it tends to add life and meaning to a subject that often overemphasizes mathematical formalism.

IV. RELATIVISTIC PROPERTIES OF GALLOPING WAVES (SCALAR CASE)

The fundamental Lorentz transformation between a space-time coordinate frame (x, ct) and an equivalent frame (x', ct') moving at velocity v along the x axis is given by[8]

$$x' = \gamma x - \beta\gamma ct\,,$$
$$ct' = -\beta\gamma x + \gamma ct\,, \tag{4.1}$$

where $\beta \equiv v/c$ and $\gamma \equiv 1/(1-\beta^2)^{1/2}$. The inverse transformation

$$x = \gamma x' + \beta\gamma ct'\,, \tag{4.2a}$$
$$ct = \beta\gamma x' + \gamma ct'\,, \tag{4.2b}$$

corresponds to simply changing the sign of the velocity (v) in (4.1) and relabeling the coordinates.

The transformations (4.1) and (4.2) can be visualized using a Minkowski grid. Minkowski plots provide a powerful graphical means for resolving many relativistic curiosities or "paradoxes." An example of a Minkowski grid for a relative velocity of one-half the speed of light ($\beta = 1/2$) is shown by the diamond grid structure in Fig. 5. To obtain this grid one uses Eqs. (4.2a) and (4.2b) to plot in (x', ct') space a series of lines corresponding to constant x and con-

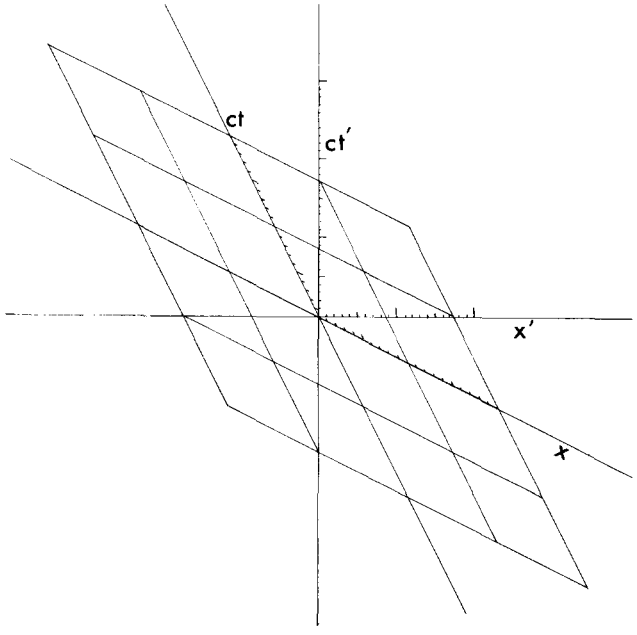

Fig. 5. Example of Minkowski grid for $v = c/2$.

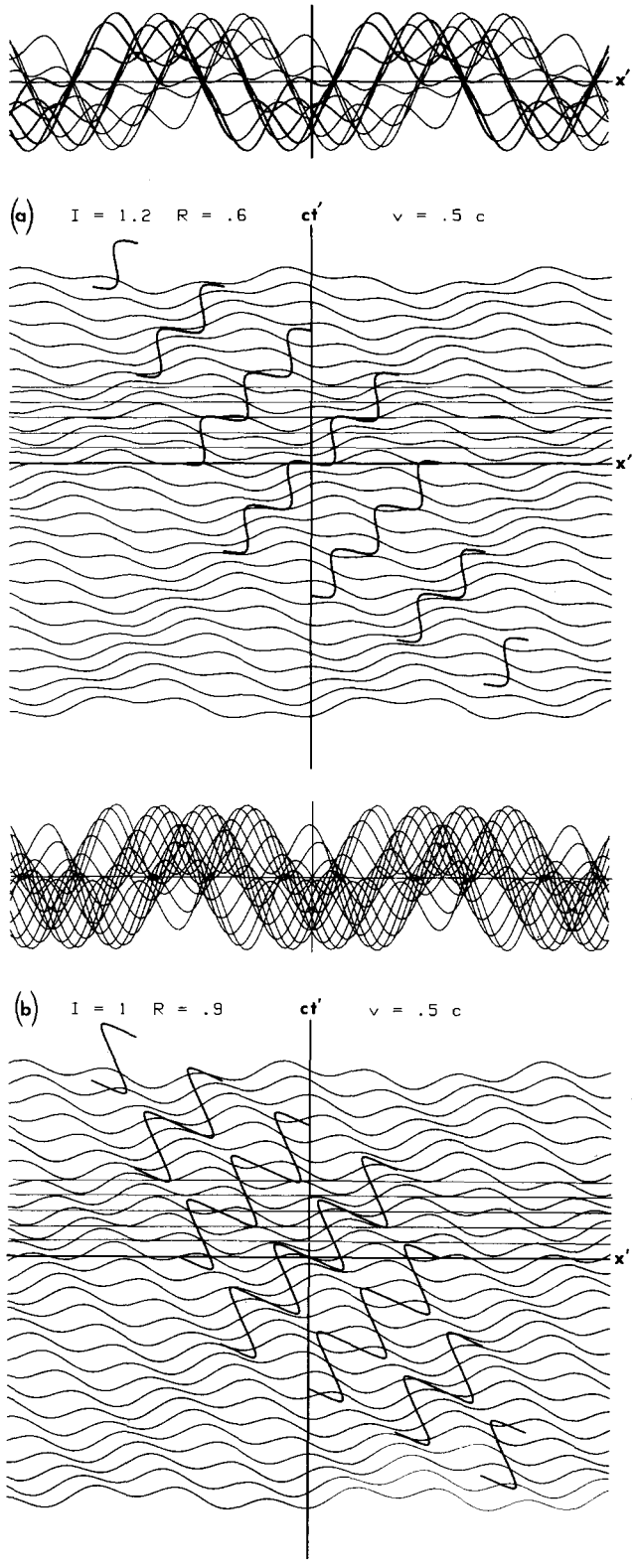

Fig. 6. (a) and (b) Trajectories of the two galloping waves from Fig. 1 are viewed from a frame moving at half the speed of light.

stant ct, respectively, for a range of constants from -2 to $+2$ in unit steps. This plot shows how the second observer would view the axes and grid of the original (x, ct) frame relative to his (x', ct') axes.

It is interesting to speculate whether such a grid could be produced physically so that an (x', ct') observer could record it. We have already noted the form of zero trajectories for galloping waves in Figs. 1 and 2. In particular, the trajectories in Fig. 1(b) approximate a grid in between their avoided crossings. The grid becomes better defined as the SWR approaches zero ($\Delta \to 0$) as shown by Fig. 2. Therefore, nearly standing waves (i.e., very rapidly galloping waves) should have zero trajectories in a moving frame that approximately follow a Minkowski grid.

These trajectories can be plotted without appealing directly to the Lorentz transformations. Instead, one may plot the sum of two counter-propagating waves with unequal frequencies directly onto a space-time (x', ct') graph. As in Sec. II, the plots are of the real part of a wave function

$$A(x', t') = Ie^{i(k_I x' - \omega_I t')} + Re^{i(k_R x' - \omega_R t')}, \tag{4.3a}$$

where incident and reflected waves both have the speed of light

$$c = \omega_I / k_I = \omega_R / k_R , \tag{4.3b}$$

but the incident wave is frequency red-shifted by a factor $\delta < 1$

$$\omega_I = \omega\delta , \tag{4.3c}$$

while the reflected wave is blue-shifted by the inverse factor

$$\omega_R = \omega/\delta . \tag{4.3d}$$

This is consistent with the Doppler shifts which will be seen by an (x', ct') observer moving at a speed $v = \beta c$ in the opposite direction of the reflected wave and in the same direction as the incident one. The Doppler shift factor is given by the following formula[8]:

$$\delta = [(1-\beta)/(1+\beta)]^{1/2} = \gamma(1-\beta) . \tag{4.4}$$

For $v = c/2$ this factor is $\delta = 1/\sqrt{3} = 0.577$. The resulting waves for $\delta = \sqrt{3}$ and their zero trajectories are plotted in Fig. 6(a) and (b) using Eq. (4.3) with the same amplitudes I and R which appear in Fig. 1(a) and (b), respectively. The superposition of wave snapshots are shown at the top of Fig. 6(a) and (b), and they are quite complicated since galloping and beating are occurring simultaneously. This is the most complicated type of nondispersive interference that two one-dimensional plane waves can have.

However, the same plots displayed on the space-time (x', ct') graphs in Fig. 6 are less complicated. One can follow the progress of the complicated wave by tracing the zero trajectories which are the solid zig-zag lines. Also, five of the snapshots just above the x' axis have constant time (t') baselines drawn in to help in locating the wave zeros. As in Fig. 1, one should view the wave amplitudes as being plotted in perspective and normal to the (x', ct') plane. The zero trajectories lie in this plane since they are the loci of points where the waves intersect the base lines of constant observer time (t') on the plane.

It is evident that each zero trajectory in Fig. 6 is not a single-valued function of the observer time (t'). There are times when a single given trajectory exists at three different positions along the x' direction. A given wave zero is uniquely located at each time (t) on the source frame (x, ct) in Fig. 1, but there are intervals of observer time (t') in which a particular zero has split into three parts as its trajectory forms a switchback in time. The time intervals for triple existence appear to be quite short in Fig. 6(a), but as the SWR(Δ) approaches zero they will become a significant fraction of an oscillation period as seen in Fig. 6(b). Also, as Δ approaches zero the switchback corners become sharper and approach the opposite corners on neighboring trajectories.

The switchback corners correspond to the avoided crossings mentioned in connection with Figs. 1 and 2. In the standing wave limit ($\Delta = 0$) these corners will close and form a Minkowski grid. The trajectories for $\Delta = 1/19$ in

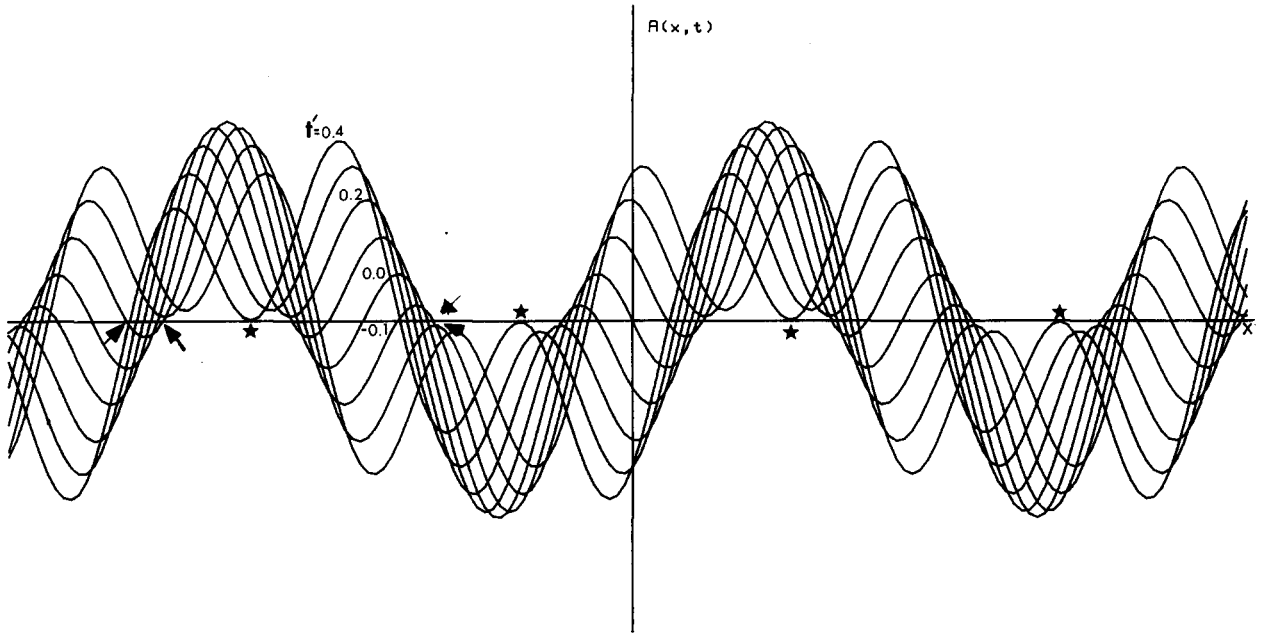

Fig. 7. More detailed superposition of the galloping wave viewed from a moving frame at equally spaced increments of time. The stars indicate the points where a pair of zeros are just being created at $t' = 0.4$. The arrows mark the location at $t = -0.1$ of pairs of zeros that were created earlier.

Fig. 6(b) are already approximately parallel to the grid lines in Fig. 5. One can view the trajectories in Fig. 6(b) as partially outlining a 4×4 diamond-shaped checkerboard in which the black squares contain waves with positive amplitude and the alternate squares contain waves with negative amplitude.

It is interesting to see how switchback corners are formed by a general galloping wave. The bottom corner of a switchback corresponds to "zero creation" whereby a pair of zeros suddenly appears on portions of the x' axis at some instant. This corresponds to a bifurcation is which an extremum point of a wave crosses the x' axis. This happens near the left-hand side of Fig. 7 between the times $t' = -0.2$ and $t' = -0.1$. This figure shows the waves of Fig. 6(b) in greater detail, and the newly created zeros are indicated by arrows at the positions they occupy at $t' = -0.1$. Both zeros proceed toward the left, but one of them moves more rapidly and is "annihilated" shortly before $t' = 0.2$. The annihilation occurs when the extreme left-hand maximum point of the wave drops below the x' axis. Zero-annihilation corresponds to the upper corners of the switchback trajectories in Fig. 6. It is followed quickly in each case by another zero creation slightly to the left. One can see zero creation just beginning at $t' = 0.4$ near points marked by stars in Fig. 7.

It appears that a moving observer might be able to record the trajectories of a perfect Minkowski grid if he passed through a source frame in which a perfect standing wave had been established. The question remains: Can this be done using mirrors with light or radio waves? So far we have discussed the case of scalar wave interference in which the amplitude invariance was tacitly assumed. In order to use electromagnetic radiation one must take account of the Lorentz transformation of the electromagnetic vector amplitudes. Vector wave interference is treated in the following section.

V. RELATIVISTIC PROPERTIES OF GALLOPING LIGHT WAVES

We consider two counterpropagating electromagnetic waves described by the incident wave electric and magnetic fields $[E_i(x,t), B_i(x,t)]$ and reflected wave fields $[E_r(x,t), B_r(x,t)]$ in the source frame. We will suppose that the electric E fields only oscillate in the y direction and the magnetic B fields only oscillate in the z direction as shown in Fig. 8. We also suppose that at $x = 0 = t$ the fields $E_i = I$ and $E_r = R$ are in phase so that the electric wave function

$$E_y = E(x,t) = Ie^{i(kx-\omega t)} + Re^{-i(kx+\omega t)} \tag{5.1}$$

has the same form as the scalar wave did in Eq. (2.2). However, Maxwell's equations require that the magnetic wave function then have the form

$$B_z = B(x,t) = Ie^{i(kx-\omega t)} - Re^{-i(kx+\omega t)}, \tag{5.2}$$

as shown in Fig. 8. (The fields are given in cgs units.)

With these assumptions it follows that the galloping velocity of the electric zero points is given by the same formulas (2.5) that are applied to scalar wave zeros. The magnetic zero points are found to have a galloping velocity that is phase shifted by $\pi/2$.

$$v_{\text{zero}}(B) = c\Delta/[\Delta^2 + (1-\Delta^2)\cos^2(\omega t + \pi/2)]\,. \tag{5.3}$$

Hence the B wave gallops while the E wave rests, and vice versa, so that the propagation resembles a game of leapfrog.

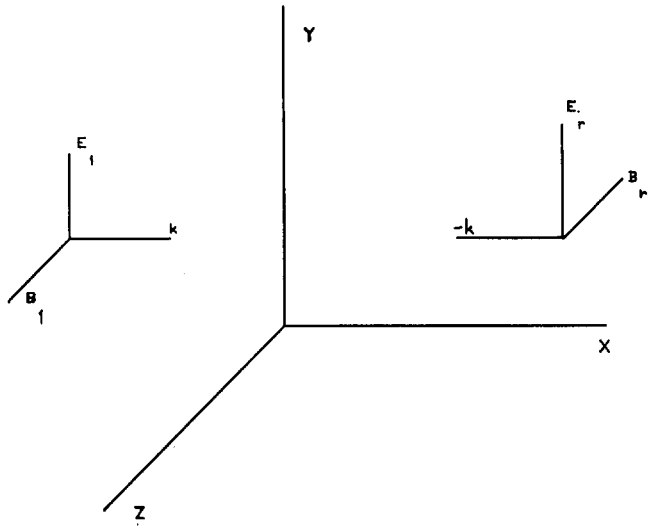

Fig. 8. Coordinates used for describing the reflected and incident vector waves.

We consider now the Lorentz transformation from the quantities in the source frame (x, ct) wave field to the values which would be observed in a frame (x', ct') moving at velocity $v = \beta c$ down the x axis. We need to find all the primed quantities in the expressions[8]

$$E'(x',t') = I'_E\, e^{i(k_I x' - \omega_I t')} + R'_E\, e^{-i(k_R x' + \omega_R t')},$$
$$B'(x',t') = I'_B\, e^{i(k_I x' - \omega_I t')} + R'_B\, e^{-i(k_R x' + \omega_R t')}, \tag{5.4}$$

in terms of source quantities. The wavenumber and angular frequencies $(k, \omega/c)$ transform just like (x, ct) in Eqs. (4.1) and (4.2). For the incident wave one has[8]

$$k_I = \gamma k - \beta\gamma\omega/c = \gamma(1-\beta)k\,,$$
$$\omega_I = -\beta\gamma ck + \gamma\omega = \gamma(1-\beta)\omega\,, \tag{5.5}$$

and for the reflected wave one has

$$k_R = \gamma k + \beta\gamma\omega/c = \gamma(1+\beta)k\,,$$
$$\omega_R = \beta\gamma ck + \gamma\omega = \gamma(1+\beta)\omega\,. \tag{5.6}$$

This yields the Doppler-shifted electric waves

$$E'(x',t') = I'_E\, e^{i(x'-ct')k\delta} + R'_E\, e^{-i(x'+ct')k/\delta}, \tag{5.7}$$

where δ was given by Eq. (4.4) and a similar expression for the magnetic waves.

To derive the field amplitudes one may use the Lorentz transformation[8]

$$F^{\alpha\beta'} = \Lambda^{\alpha}_{\mu}\, F^{\mu\nu}\, \Lambda^{\beta}_{\nu} \tag{5.8}$$

of the field tensor

$$\langle F^{\mu\nu}\rangle = \begin{pmatrix} \cdot & \cdot & -E_y & \cdot \\ \cdot & \cdot & -B_z & \cdot \\ E_y & B_z & \cdot & \cdot \\ \cdot & \cdot & \cdot & \cdot \end{pmatrix}, \tag{5.9}$$

where

$$\langle \Lambda^{\alpha}_{\mu}\rangle = \begin{pmatrix} \gamma & \beta\gamma & \cdot & \cdot \\ -\beta\gamma & \gamma & \cdot & \cdot \\ \cdot & \cdot & 1 & \cdot \\ \cdot & \cdot & \cdot & 1 \end{pmatrix}. \tag{5.10}$$

The result of the transformation is very simple. The new

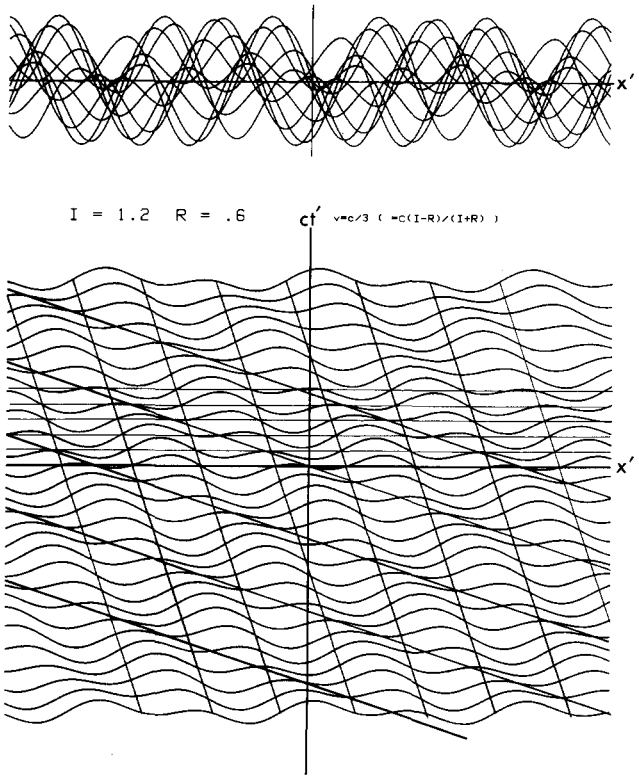

Fig. 9. Space-time zero-point trajectories for a vector wave in a frame in which it has stopped galloping. In this case the zero-point trajectories follow the coordinate lines of a Minkowski grid.

incident amplitudes are

$$I'_E = I'_B = \gamma(1-\beta)I = I\delta\,, \tag{5.11}$$

and the new reflected amplitudes are

$$R'_E = R'_B = \gamma(1+\beta)R = R/\delta\,. \tag{5.12}$$

In other words, the amplitudes are each multiplied or divided by the same Doppler shift fraction $\delta = [(1-\beta)/(1+\beta)]^{1/2}$ that appears in the frequency and wavenumber transformations (5.5) and (5.6).

If the ratio of the source amplitudes I and R differs from unity but is finite then there exists a moving frame in which the amplitudes I' and R' are equal. This is the frame for which the Doppler fraction is

$$\delta = \sqrt{R}/\sqrt{I}\,. \tag{5.13}$$

This yields the equation

$$(1-\beta)/(1+\beta) = R/I\,. \tag{5.14}$$

Solving this equation one finds that the velocity parameter for this frame is

$$\beta \equiv v/c = (I-R)/(I+R)\,, \tag{5.15}$$

and this is just the source frame SWR(Δ) defined in Eq. (2.1).

This shows how to broadcast a radio, radar, or light signal which would produce an observable Minkowski frame for a moving observer capable of recording the trajectories of electric field zero points. The source frame (x, ct) must set up a galloping wave with an SWR equal to the moving observer's velocity in units of c. Figure 9 shows the E waves and zero trajectories for an observer moving at one third the speed of light ($\beta = 1/3$) through a source wave similar to Fig. 1(a) for which $\Delta = 1/3$. As in previous figures, baselines or constant-t' lines are drawn to confirm the location of zeros for five snapshots. The zero trajectories are all straight lines which represent space and time grid lines of the source frame.

It is possible to interpret the zero trajectories of the observer's E' wave in simpler terms. This may be done by rewriting the E' wave.

$$E'(x't') = (IR)^{1/2}(e^{i(k_I x' - \omega_I t')} + e^{-i(k_R x' + \omega_R t')})\,. \tag{5.16}$$

Using sum and difference quantities,

$$k_M = (k_R - k_I)/2, \quad k_C = (k_R + k_I)/2\,,$$
$$\omega_M = (\omega_R + \omega_I)/2, \quad \omega_C = (k_R - k_I)/2\,. \tag{5.17}$$

The resulting wave function is

$$E'(x't') = (IR)^{1/2} e^{-i(k_M x' + \omega_M t')} \times (e^{i(k_C x' + \omega_C t')} + e^{i(k_C x' + \omega_C t')})\,,$$

for which the real part

$$\mathrm{Re}\,E'(x't') = 2(IR)^{1/2}\cos(k_M x' + \omega_M t') \times \cos(k_C x' + \omega_C t') \tag{5.18}$$

has the form of one wave modulating another. The first wave factor has wavelength $\lambda_M = 2\pi/k_M$ and frequency ω_M where from Eqs. (5.5), (5.6), and (5.17) we have

$$k_M = \beta\gamma\omega/c, \quad \omega_M = \gamma\omega\,. \tag{5.19}$$

The second wave factor has a shorter wavelength $\lambda_C = 2\pi/k_C = \lambda_M\beta$ and a lower frequency $\omega_C = \omega_M\beta$, where

$$k_C = \gamma\omega/c, \quad \omega_C = \beta\gamma\omega\,. \tag{5.20}$$

We shall refer to it as the "carrier" which is being modulated by the first wave factor.

The velocities of the two wave factors are given by

$$\begin{aligned} v_C &= -\omega_C/k_C \quad v_M = -\omega_M/k_M \\ &= -\beta c\,, \qquad\quad = -c/\beta\,. \end{aligned} \tag{5.21}$$

One can see in Fig. 9 that the zeros of the slow-moving carrier wave determine the x lines of the Minkowski grid which have a slope of $-\beta = -1/3$ in the (x', ct') graph. There are three of these carrier zeros for each one of the modulation wave zeros. The modulation zeros determine the t lines of the Minkowski grid. The modulation moves toward the left at three (i.e., $1/\beta$) times the speed of light in Fig. 9.

This amounts to a rather spectacular form of wave interference which becomes even more so as β (and Δ) approach zero. For example, the $\beta = 1/100$ observer would see 100 waves in each beat or modulation pattern moving at a velocity of $-c/100$. Meanwhile the enveloping or modulating wave would be racing along uniformly at a velocity of $-100c$. However, the source frame observes a very nonuniformly galloping wave whose velocity varies between $+c/100$ and $+100c$.

VI. ADDITIONAL TOPICS

After considering the details of one-dimensional interference it may be worthwhile to investigate equally detailed pictures of two-or three-dimensional wave propagation. Feynman[9] has shown that a very clear picture of waveguide phase and group velocity and dispersion relations can be had simply by considering a pair of obliquely propagating plane waves of equal frequency and amplitude. Combinations of such pairs give rise to much more complicated wave interference effects. These would be present in many

of the so-called "four-wave mixing" problems being studied in the field of quantum optics. They would also be related to the study of wave-front catastrophes[10] which were mentioned in the Introduction.[2]

ACKNOWLEDGMENT

One of us (WGH) would like to thank the National Science Foundation for support from Grant PHY-8207150 theoretical physics.

[1]In Halliday and Resnik, for example, the only mention of this sort of interference is in two problems which involve SWR calculations.

[2]M. V. Berry, F.R.S., Proc. R. Soc. London Ser. A **336**, 165 (1974).

[3]R. P. Feynman, *Quantum Electrodynamics* (Benjamin, New York, 1960).

[4]I. I. Rabi, N. F. Ramsey, and J. Schwinger, Rev. Mod. Phys. **26**, 167 (1954).

[5]R. P. Feynman, F. L. Vernon, and R. W. Hellwarth, J. Appl. Phys. **28**, 49 (1957).

[6]W. G. Harter and N. dos Santos, Am. J. Phys. **46**, 251 and 264 (1978).

[7]R. P. Feynman, R. B. Leighton, and M. Sands, *The Feynman Lectures in Physics* (Addison-Wesley, Reading, MA, 1965), Vol. III, pp. 8–11, 14. See Fig. 8-2.

[8]J. D. Jackson, *Classical Electrodynamics* (Wiley, New York, 1975), Chap. 11.

[9]Reference 7, Vol. II, pp. 24-10, 13. See Fig. 24-17.

[10]M. V. Berry, Adv. Phys. **25**, 1 (1976); see also J. Walker's column in Sci. Am. **249** (3), 190 (Sept. 1983).

Illustration of resonances and the law of exponential decay in a simple quantum-mechanical problem

Herbert Massmann

Universidad de Chile, Casilla 653, Santiago, Chile

(Received 14 December 1983; accepted for publication 7 July 1984)

The exact quantum-mechanical solution of a particle moving in a one-dimensional well formed by a delta barrier in front of an impenetrable well is used to illustrate the relation between scattering resonances and exponential decay from the well.

I. INTRODUCTION

The purpose of this contribution is to illustrate the resonance phenomena and the law of exponential decay in a very simple one-dimensional quantum-mechanical problem: a mass μ moving in a potential given by (see also Fig. 1)

$$V(x)=\begin{cases}\infty & x<0\\ W_0\delta(x-x_0) & x\geqslant 0\end{cases}. \tag{1}$$

The δ function in the potential can be considered as a square barrier of height h and width l in the limit $l\to 0$, $h\to\infty$ such that the product $hl=W_0$ remains constant. Without changing the essential features of the problem, the use of the δ function considerably reduces the algebra in the process of solving the Schrödinger equation, since one will effectively have to consider only two regions (region I and II) instead of three which would be the case if a finite barrier is considered. This simplification introduced by δ functions has been exploited in numerous occasions mainly in problems used for pedagogical purposes.[1] A few cases, published recently in this journal, applied to bound state problems and scattering situations and are given in Refs. 2 and 3, respectively.

In Sec. II the time-independent Schrödinger equation with the potential given by Eq. (1) will be solved for a scattering type situation, that is, for the case in which a particle of energy E and mass μ will be incident from the right onto the δ barrier. Resonance phenomena are readily found; for certain energies the probability that the particle penetrates into region I will increase enormously. These resonances, in the limit in which the transmission through the δ barrier is small, have the familiar Breit–Wigner shape[4] (Sec. III). In this way, a simple expression for the width Γ_n of the resonance (or quasistationary state) is found.

In Sec. IV it is assumed that for $t=0$ the particle is trapped inside the well (region I) in a specific state, and the time evolution of this state will be considered. In particular, it is shown that the probability of finding the particle in region I decays according to the exponential law $P(t)=\exp(-t/\tau_n)$. It turns out, as expected, that the mean life τ_n is related to the width Γ_n of the quasistationary state

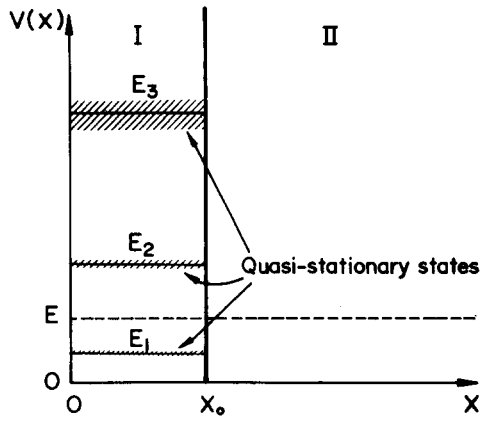

Fig. 1. Diagram of the potential.